



E2022014

2022-08-16

Good Volatility, Bad Volatility, and VIX Futures Pricing: Evidence from the Decomposition of VIX

Chen Tong
Zhuo Huang

Abstract

Realized semivariance, computed from intraday positive/negative squared returns, provides an accurate measure of the upside/downside variations of stock returns. This paper investigates the role of realized semivariance in pricing the CBOE VIX and VIX futures, using a realized semivariance-based model. We obtain the closed-form pricing formula for the VIX index and VIX futures prices, and show that the new model provides superior pricing performance, both in-sample and out-of-sample. We further analytically derive the pricing formulas for the upside/downside components of the VIX (risk-neutral semivariance). Such a decomposition shows that the information gains from the conventional unsigned realized variance are concentrated on pricing the downside part of the VIX, while the new realized semivariance-based model provides a larger and more balanced improvement for both the upside and downside components of the VIX. Our results provide strong evidence that the spread between upside/downside variance is the main driver of the asymmetry in return distributions.

Keywords: Realized semivariance, VIX futures, VIX decomposition, Risk-neutral semivariance

JEL Classification: G12, G13, C51, C52

*Corresponding author: Chen Tong (tongchen@xmu.edu.cn). Zhuo Huang acknowledges financial support from the National Natural Science Foundation of China (71671004). Chen Tong acknowledges financial support from the Ministry of Education of China, Humanities and Social Sciences Youth Fund (XXXXXX) and the Fundamental Research Funds for the Central Universities (20720221025).

Good Volatility, Bad Volatility, and VIX Futures Pricing: Evidence from the Decomposition of VIX

Chen Tong^{a*} Zhuo Huang^b

*^aDepartment of Finance, School of Economics & Wang Yanan Institute
for Studies in Economics (WISE), Xiamen University, China*

^bNational School of Development, Peking University, China

August 11, 2022

Abstract

Realized semivariance, computed from intraday positive/negative squared returns, provides an accurate measure of the upside/downside variations of stock returns. This paper investigates the role of realized semivariance in pricing the CBOE VIX and VIX futures, using a realized semivariance-based model. We obtain the closed-form pricing formula for the VIX index and VIX futures prices, and show that the new model provides superior pricing performance, both in-sample and out-of-sample. We further analytically derive the pricing formulas for the upside/downside components of the VIX (risk-neutral semivariance). Such a decomposition shows that the information gains from the conventional unsigned realized variance are concentrated on pricing the downside part of the VIX, while the new realized semivariance-based model provides a larger and more balanced improvement for both the upside and downside components of the VIX. Our results provide strong evidence that the spread between upside/downside variance is the main driver of the asymmetry in return distributions.

Keywords: Realized semivariance, VIX futures, VIX decomposition, Risk-neutral semivariance

JEL Classification: G12, G13, C51, C52

*Corresponding author: Chen Tong (tongchen@xmu.edu.cn). Zhuo Huang acknowledges financial support from the National Natural Science Foundation of China (71671004). Chen Tong acknowledges financial support from the Ministry of Education of China, Humanities and Social Sciences Youth Fund (XXXXXX) and the Fundamental Research Funds for the Central Universities (20720221025).

1 Introduction

The Chicago Board Options Exchange (CBOE) VIX index, computed from S&P 500 index (SPX) options prices, is a model-free measure of the expected average variance for the next 30 days under the risk-neutral measure. CBOE introduced VIX futures in 2004 and VIX options in 2006, to enable investors to directly trade volatility. Because of a negative correlation¹ between changes in the VIX and the SPX, market participants treat VIX derivatives as an important trading vehicle for reducing exposure to risk. Because of the boom in VIX-linked products, much academic attention has been devoted to finding an accurate valuation model for VIX derivatives.

It is well known that realized measures of volatility, computed from high-frequency intraday data, provide accurate measurements of latent volatility processes. Many studies have highlighted the importance of realized variance in volatility forecasting² and derivatives pricing.³ In recent years, advances in variance analysis (Barndorff-Nielsen et al., 2010) have made it possible to split conventional realized variance into upside and downside semivariances, which are respectively obtained by summing the intraday positive and negative squared returns. Many studies have established that this decomposition enhances volatility predictions (Patton & Sheppard, 2015), index option pricing (Feunou & Okou, 2019), and highlighted the upside/downside variance spread as a source of the asymmetry in stock price distributions (Feunou et al., 2011). The main goal of this paper is to investigate the role of realized semivariance in pricing the CBOE VIX index and VIX futures, from a decomposition perspective.

The key step in pricing VIX derivatives is to derive the model-implied VIX pricing formula. The theoretical foundation of the model-free algorithm of the CBOE VIX can be traced back to Britten-Jones & Neuberger (2000). More recently, Andersen et al. (2015) argued that the CBOE VIX is actually an approximation of Model-Free Implied Volatility (MFIV), which is a special case of Corridor Implied Volatility (CIV) without truncations. Based on this concept, Andersen & Bondarenko (2007) proposed the risk-neutral semivariances constructed by call and put options, respectively. This approach forms the foundation for decomposing the VIX into upside and downside components. Many empirical studies have documented the asymmetric effects of these two VIX components in asset pricing. One prominent example is the study by Feunou et al. (2017), who constructed the upside/downside variance risk premium (VRP) based on the difference between risk-neutral

¹The correlation between the daily log change of the VIX and the SPX was -73% from 2000 to 2020.

²These include Hansen et al. (2012, 2016), Engle & Gallo (2006), Shephard & Sheppard (2010).

³See e.g. Corsi et al. (2013), Christoffersen et al. (2014), Majewski et al. (2015), Huang et al. (2017), Tong et al. (2022) for index option pricing, and Huang et al. (2019), Wang & Wang (2021), Tong & Huang (2021) for VIX derivatives pricing.

and realized semivariance. They established that the downside VRP is the main component of the VRP. [Dotsis & Vlastakis \(2016\)](#) found that only the upside VIX component carries a significant negative risk premium in the cross-section of stock returns, and it subsumes all relevant information for forecasting future volatility. Other related studies include [Kilic & Shaliastovich \(2019\)](#), [Fu et al. \(2016\)](#) and [Held et al. \(2020\)](#).

Despite the extensive literature on VIX pricing, little attention has been paid to the model's ability to price different VIX components. As mentioned above, the upside and downside components of the VIX display distinct empirical performance, and these differences may come from asymmetries in the distribution of the underlying asset. In this paper, we model the underlying process using a realized semivariance-based model, the generalized skew affine realized variance (GSARV) of [Feunou & Okou \(2019\)](#), in which the asset price features specific upside (good) and downside (bad) variance dynamics. We obtain the closed-form pricing formulas for both the CBOE VIX index and VIX futures, and show that models with realized semivariance provide superior pricing performance, both in-sample and out-of-sample. To identify the source of these improvements, we further analytically derive the model-implied pricing formulas for both the upside and downside components of the VIX (i.e., risk-neutral semivariance). Such a decomposition of the VIX shows that the information gains from the conventional unsigned realized variance are concentrated on the pricing of the downside part of the VIX, while the new model incorporating signed realized semivariance provides a larger and more balanced improvement in both the upside and downside components of the VIX. Our results provide strong evidence that the spread between upside/downside variance is the main driver of the asymmetry in stock price distributions.

We contribute to the literature on VIX derivatives pricing with realized measures of volatility. [Huang et al. \(2019\)](#) were the first to focus on pricing VIX derivatives using realized variance. They used an extended LHARG model ([Majewski et al., 2015](#)) to price the VIX futures and showed that realized variance significantly improves the model's pricing performance. [Wang & Wang \(2021\)](#) used the GARV model ([Christoffersen et al., 2014](#)) to price VIX futures. More recently, [Tong & Huang \(2021\)](#) emphasized the importance of realized variance in pricing VIX options using the realized GARCH model ([Hansen et al., 2012](#)) and the GARV model. Our paper is closely related to that of [Qiao et al. \(2022\)](#), who focused on the forecasting power of realized semivariance for the VIX term structure. However, their model specifications did not allow for conditional skewness in the return distribution, as they imposed Gaussian innovations. We make additional contributions to this strand of the literature by developing a generalized VIX futures pricing model based on realized semivariance, and showing that allowing for distinct up/down variance dynamics

is useful in pricing the CBOE VIX and its futures from a decomposition perspective.

The rest of this paper is organized as follows. In Section 2, we introduce the GSARV model and its risk-neutral dynamics. In Section 3, we present the theoretical foundations for the CBOE VIX and its decomposition. Section 4 shows how to analytically derive the model-implied pricing formulas for the VIX, VIX components, and VIX futures. Section 5 displays the competing models for comparison. Section 6 describes the estimation method. All of the empirical results are reported in Section 7, including summary statistics, parameter estimates, and in-sample and out-of-sample pricing performance. All of the relevant proofs are given in the appendix.

2 Model

2.1 The Realized Semivariance

Advances in variance analysis have made it possible to split the total quadratic variation into upside and downside components using intraday returns. According to [Bardorff-Nielsen et al. \(2010\)](#), the upside/downside realized variances for a given day t are given by

$$\begin{aligned} RV_t^U &= \sum_{j=1}^{n_t} r_{t,j}^2 \mathbb{I}_{[r_{t,j}>0]} \\ RV_t^D &= \sum_{j=1}^{n_t} r_{t,j}^2 \mathbb{I}_{[r_{t,j}<0]} \end{aligned}$$

where $r_{t,j} = \log(S_{t,j}/S_{t,j-1})$ is the j -th observation of intraday returns, n_t is the number of observations on day t , and $\mathbb{I}_{[*]}$ is the indicator function. The sum of RV_t^U and RV_t^D is the traditional realized variance denoted by RV_t . If we assume that the following jump-diffusion motion

$$d \log S_t = \mu_t dt + \sigma_t dW_t + J_t$$

where dW_t is an increment of standard Brownian motion and $J_t = \log(S_t/S_{t-})$ refers to the jump component; then when n_t goes to infinity, the realized measures will converge to

$$\begin{aligned} RV_t^U &\xrightarrow{P} \frac{1}{2} \int_{t-1}^t \sigma_s^2 ds + \sum_{t-1 \leq s \leq t} J_s^2 \mathbb{I}_{[J_s > 0]} \\ RV_t^D &\xrightarrow{P} \frac{1}{2} \int_{t-1}^t \sigma_s^2 ds + \sum_{t-1 \leq s \leq t} J_s^2 \mathbb{I}_{[J_s < 0]} \end{aligned}$$

Thus, the difference between RV_t^U and RV_t^D can be interpreted as a measure of skewness:

$$RV_t^U - RV_t^D \xrightarrow{P} \sum_{t-1 < s \leq t} J_s^2 (\mathbb{I}_{[J_s > 0]} - \mathbb{I}_{[J_s < 0]})$$

and if $RV_t^U - RV_t^D < 0$, the distribution is left-skewed, and when $RV_t^U - RV_t^D > 0$, it is right-skewed. A more detailed theoretical justification is given by [Feunou et al. \(2016\)](#).

2.2 GSARV Model

We use the GSARV model of [Feunou & Okou \(2019\)](#) to incorporate the realized semivariance into the modeling of stock returns. It is given by

$$R_{t+1} = \bar{r} + (\lambda_u - \xi_u) h_{u,t+1} + (\lambda_d - \xi_d) h_{d,t+1} + z_{u,t+1} - z_{d,t+1}$$

where the innovation to daily log returns $R_{t+1} = \log(S_{t+1}/S_t)$ consists of two components, $z_{u,t+1}$ and $z_{d,t+1}$, representing the positive and negative shocks, respectively. The component $z_{j,t+1}$, $j = \{u, d\}$ is assumed to follow a demean non-central χ^2 distribution with conditional variance $\text{var}_t(z_{j,t+1}) = h_{j,t+1}$:

$$z_{j,t+1} = \sqrt{\frac{\omega_j}{2}} \left(\varepsilon_{j,t+1}^2 - 1 - 2\varepsilon_{j,t+1} \sqrt{\frac{h_{j,t+1} - \omega_j}{2\omega_j}} \right), \quad \varepsilon_{j,t+1} \stackrel{\text{iid}}{\sim} \text{N}(0, 1)$$

Therefore, the conditional variance h_{t+1} for daily log return R_{t+1} has two components:

$$h_{t+1} \equiv \text{var}_t(R_{t+1}) = h_{u,t+1} + h_{d,t+1}$$

which can be interpreted as good and bad stock market volatilities, and the parameters λ_u and λ_d represents the market price of upside/downside risk⁴. The conditional skewness of log returns is time-varying and given by

$$\text{skew}_t(R_{t+1}) = \frac{h_t^{-3/2}}{\sqrt{2}} \left[3\sqrt{\omega_u} (h_{u,t} - h_{d,t}) + 3(\sqrt{\omega_u} - \sqrt{\omega_d}) h_{d,t} - (\omega_u^{3/2} - \omega_d^{3/2}) \right].$$

Therefore, two sources of conditional asymmetry emerge: i) the discrepancy between non-normality in good and bad shock distributions $\sqrt{\omega_u} - \sqrt{\omega_d}$ and ii) the difference between upside and downside variance $h_{u,t} - h_{d,t}$.

Realized semivariance, $RV_{j,t}$, is linked to the conditional variance through the following

⁴The reason is that the expected return is given by $\mathbb{E}_t(\exp(R_{t+1})) = \exp(r + \lambda_u h_{u,t+1} + \lambda_d h_{d,t+1})$. Please see [Feunou & Okou \(2019, Equation 9\)](#) for more details.

measurement equation:

$$RV_{j,t} = h_{j,t} + \sigma_j \left[\left(v_{j,t} - \gamma_j \sqrt{h_{j,t} - \omega_j} \right)^2 - 1 - \gamma_j^2 (h_{j,t} - \omega_j) \right], \quad v_{j,t} \stackrel{\text{iid}}{\sim} N(0, 1)$$

This also introduces the volatility specific shock $v_{j,t}$, which can be used to update the dynamics of each component of the conditional variances:

$$h_{j,t+1} - \omega_j = \bar{\omega}_j + \beta_j (h_{j,t} - \omega_j) + \alpha_j \left(v_{j,t} - \gamma_j \sqrt{h_{j,t} - \omega_j} \right)^2$$

where the parameter γ_j captures the nonlinear impact of a volatility shock on RV_t^j . The dependence for different innovations is specified as

$$\begin{aligned} \mathbb{E}_t [\boldsymbol{\varepsilon}_{u,t+1} \boldsymbol{\varepsilon}_{d,t+1}] &= 0, \\ \mathbb{E}_t [v_{u,t+1} v_{d,t+1}] &= 0, \\ \mathbb{E}_t [\boldsymbol{\varepsilon}_{j,t+1} v_{j,t+1}] &= \rho_j. \end{aligned}$$

2.3 Risk Neutralization

Feunou & Okou (2019) proposed the following exponential pricing kernel to risk-neutralize the GSARV model:

$$M_{t,t+1} = M_{t,t+1}^{(u)} M_{t,t+1}^{(d)}$$

where

$$M_{t+1}^{(j)} = \frac{\exp \left(\theta_{1t}^{(1j)} \boldsymbol{\varepsilon}_{j,t+1} + \theta_2^{(1j)} \boldsymbol{\varepsilon}_{j,t+1}^2 + \theta_{1t}^{(2j)} v_{j,t+1} + \theta_2^{(2j)} v_{j,t+1}^2 \right)}{\mathbb{E}_t \left[\exp \left(\theta_{1t}^{(1j)} \boldsymbol{\varepsilon}_{j,t+1} + \theta_2^{(1j)} \boldsymbol{\varepsilon}_{j,t+1}^2 + \theta_{1t}^{(2j)} v_{j,t+1} + \theta_2^{(2j)} v_{j,t+1}^2 \right) \right]}$$

for $j = \{u, d\}$. They showed that the risk-neutral dynamics of the GSARV model are given by

$$\begin{aligned} R_{t+1} &= \bar{r}^* - \xi_u^* h_{u,t+1}^* - \xi_d^* h_{d,t+1}^* + z_{u,t+1}^* - z_{d,t+1}^* \\ h_{j,t+1}^* - \omega_j^* &= \bar{\omega}_j^* + \beta_j (h_{j,t}^* - \omega_j^*) + \alpha_j^* \left(v_{j,t}^* - \gamma_j^* \sqrt{h_{j,t}^* - \omega_j^*} \right)^2 \end{aligned}$$

Feunou & Okou (2019) did not explicitly derive the measurement equation linking the RV_t^j to $h_{j,t}^*$ in risk-neutral measure. In Appendix E, we show that it has the following expression:

$$RV_{j,t}^* = h_{j,t}^* + \sigma_j^* \left[\left(v_{j,t}^* - \gamma_j^* \sqrt{h_{j,t}^* - \omega_j^*} \right)^2 - 1 - \gamma_j^{*2} (h_{j,t}^* - \omega_j^*) \right]$$

where $RV_{j,t}^*$ is defined by $RV_{j,t}^* \equiv \zeta_j^* + \phi_j^* RV_{j,t}$ such that $\mathbb{E}_{t-1}^{\mathbb{Q}}(RV_{j,t}^*) = h_{j,t}^*$, so the parameters ζ_j^* and ϕ_j^* control the magnitude of the VRP. Then a measure of the unconditional VRP is simply given by

$$\text{VRP}_j \equiv \mathbb{E}^{\mathbb{P}}(RV_{j,t}^*) - \mathbb{E}^{\mathbb{P}}(RV_{j,t}) = \zeta_j^* + (\phi_j^* - 1) \mathbb{E}^{\mathbb{P}}(RV_{j,t}).$$

Theoretically, we expect investors to like good uncertainty (because it increases the potential for substantial gains) but dislike bad uncertainty (as it increases the likelihood of severe losses), which means that VRP_u is negative and VRP_d is positive.

3 The CBOE VIX and its Decomposition

Since 2003, the VIX index reported by CBOE has shifted from Black-Scholes implied volatility to model-free implied volatility (MFIV), which does not rely on a particular option pricing model. As shown in [Jiang & Tian \(2005\)](#), the VIX is designed to approximate MFIV, as follows:

$$\left(\frac{\text{VIX}}{100}\right)^2 \times \frac{T}{365} \rightarrow \text{MFIV} \equiv 2e^{rT} \int_0^{+\infty} \frac{M_0(K)}{K^2} dK.$$

where T is the number of (calendar) days to maturity, r is the associated risk-free rate, and $M_0(K)$ is the price for an out-of-the-money (OTM) option. According to the CBOE white paper⁵, the CBOE VIX is a weighted portfolio of OTM calls and puts, given by

$$\left(\frac{\text{VIX}}{100}\right)^2 \times \frac{T}{365} = \underbrace{2e^{rT} \sum_{j=1}^N \frac{\Delta K_j}{K_j^2} M_0(K_j)}_{\text{Discrete Approximation}} - \underbrace{\left[\frac{F}{K_f} - 1\right]^2}_{\text{Correction Term}} \quad (1)$$

where F is the forward index level, K_f is the first strike below F , K_i is the strike price of the i -th OTM option, ΔK_i is the interval between strike prices, $M_0(K_i)$ is the price for each option using the midpoint of the bid-ask spread. The second term in Equation (1) adjusts for the lack of clean separation between the put and call options, arising from the discrepancy between K_f and the forward price.⁶ To obtain the VIX index for a specific maturity, e.g., 30 days, CBOE uses the interpolation of volatility calculated with near-term and next-term options. Therefore, the targeted MFIV used in CBOE is an integral with respect to the prices of OTM options.

⁵<https://cdn.cboe.com/resources/futures/vixwhite.pdf>

⁶In Appendix A, we provide a more detailed description of how the correction term emerges.

3.1 MFIV: Theoretical Arguments

Let F_t be a martingale process in risk-neutral measure, defined as the forward price $F_t = S_t e^{r(T-t)}$. Then according to [Bakshi & Madan \(2000\)](#) and [Carr & Madan \(2001\)](#), for any function $g(F)$ whose second derivative $g''(F)$ is continuous almost everywhere, we have

$$\begin{aligned}\mathbb{E}_0^{\mathbb{Q}}[g(F_T)] - g(F_0) &= e^{rT} \int_0^{F_0} g''(K) P_0(K) dK + e^{rT} \int_{F_0}^{\infty} g''(K) C_0(K) dK \\ &= e^{rT} \int_0^{+\infty} g''(K) M_0(K) dK\end{aligned}\quad (2)$$

where $\mathbb{E}_0^{\mathbb{Q}}(\cdot)$ takes the expectation under risk-neutral measure \mathbb{Q} , and $P_0(K)$ and $C_0(K)$ are the current prices of OTM puts and calls. The last equality is obtained through a put-call parity with $M_0(K) \equiv \min[P_0(K), C_0(K)]$. In addition, when we take $g(F) = \log(F)$, MFIV is related to an expectation linked to the future cumulative log return:

$$\text{MFIV} \equiv 2e^{rT} \int_0^{+\infty} \frac{M_0(K)}{K^2} dK = -2\mathbb{E}_0^{\mathbb{Q}}[\log(F_T/F_0)].\quad (3)$$

If we assume that there is a pure diffusion process for the martingale process F_t , i.e.

$$dF_t/F_t = \sigma_t dW_t,\quad (4)$$

where W_t is a standard Brownian motion and σ_t is a strictly positive, càdlàg (i.e., right-continuous with left limits) stochastic volatility process, then by Ito's Lemma, we have

$$\mathbb{E}_0^{\mathbb{Q}}[g(F_T)] - g(F_0) = \frac{1}{2} \mathbb{E}_0^{\mathbb{Q}} \left[\int_0^T g''(F_t) F_t^2 \sigma_t^2 dt \right]\quad (5)$$

When $g(F) = \log(F)$, combining Equation (2) and (5) yields

$$\mathbb{E}_0^{\mathbb{Q}}[\log(F_T/F_0)] = -\frac{1}{2} \mathbb{E}_0^{\mathbb{Q}} \left[\int_0^T \sigma_t^2 dt \right] = -e^{rT} \int_0^{+\infty} \frac{M_0(K)}{K^2} dK.$$

Thus, if the price follows the pure diffusion process in Equation (4), the VIX index reported by CBOE approximates the MFIV defined as the expected total return variation.

$$\text{MFIV} = \mathbb{E}_0^{\mathbb{Q}} \left[\int_0^T \sigma_t^2 dt \right]\quad (6)$$

3.2 VIX Decomposition: Risk-Neutral Semivariance

To decompose the CBOE VIX index (or MFIV), we resort to the definition of corridor implied volatility (CIV) proposed by [Andersen et al. \(2015\)](#)

$$\text{CIV} \equiv 2e^{rT} \int_{B_L}^{B_H} \frac{M_0(K)}{K^2} dK$$

A special case of CIV is when the barriers (B_H, B_L) take (F_0, ∞) or $(0, F_0)$, we have

$$\text{CIV}^U \equiv 2e^{rT} \int_{F_0}^{\infty} \frac{M_0(K)}{K^2} dK = 2e^{rT} \int_{F_0}^{\infty} \frac{C_0(K)}{K^2} dK \quad (7)$$

$$\text{CIV}^D \equiv 2e^{rT} \int_0^{F_0} \frac{M_0(K)}{K^2} dK = 2e^{rT} \int_0^{F_0} \frac{P_0(K)}{K^2} dK \quad (8)$$

These two measures are proposed by [Andersen & Bondarenko \(2007\)](#). As MFIV can be defined as CIV when the barriers (B_H, B_L) take $(0, \infty)$, we have the following decomposition

$$\text{MFIV} = \text{CIV}^U + \text{CIV}^D$$

An interesting finding is that CIV^U is calculated only from OTM call options and CIV^D only from OTM put options. Because the prices of call and put options reflect investors' expectations of future upward and downward market conditions, respectively, CIV^U and CIV^D may be interpreted as the upside and downside components of MFIV. To provide a deeper insight into what CIV^U actually measures, let $g(F) = \left[\frac{F}{F_0} - 1 - \ln \frac{F}{F_0} \right] \mathbb{I}_{\{F \geq F_0\}}$ and plug it into Equation (2). By doing so, we have

$$\text{CIV}^U = 2\mathbb{E}_0^{\mathbb{Q}} \left[\left(\frac{F_T}{F_0} - 1 - \ln \frac{F_T}{F_0} \right) \mathbb{I}_{\{F_T \geq F_0\}} \right] \quad (9)$$

and for CIV^D , we can take $g(F) = \left(\frac{F}{F_0} - 1 - \ln \frac{F}{F_0} \right) \mathbb{I}_{\{F \leq F_0\}}$, then it becomes

$$\text{CIV}^D = 2\mathbb{E}_0^{\mathbb{Q}} \left[\left(\frac{F_T}{F_0} - 1 - \ln \frac{F_T}{F_0} \right) \mathbb{I}_{\{F_T \leq F_0\}} \right]. \quad (10)$$

When F_t follows the diffusion process in Equation (4), combining Equations (5) and (9 or 10) yields

$$\text{CIV}^U = \mathbb{E}_0^{\mathbb{Q}} \left[\int_0^T \sigma_t^2 \mathbb{I}_{[F_t \geq F_0]} dt \right] \quad (11)$$

$$\text{CIV}^D = \mathbb{E}_0^{\mathbb{Q}} \left[\int_0^T \sigma_t^2 \mathbb{I}_{[F_t \leq F_0]} dt \right] \quad (12)$$

Therefore, CIV^U (or CIV^D) measures the expectation of the total upside (or downside) return variation when the instantaneous cumulative return $\log F_t/F_0$ is positive (or negative).

In practice, the upside/downside component of MFIV (called risk-neutral semivariance), denoted by VIX_U^2 and VIX_D^2 , can be approximated from Equations (7) and (8) by the following portfolio of OTM options:⁷

$$\left(\frac{VIX_U}{100}\right)^2 \times \frac{T}{365} \equiv 2e^{rT} \sum_{j=1}^N \frac{\Delta K_j}{K_j^2} C_0(K_j) \rightarrow CIV^U \quad (13)$$

$$\left(\frac{VIX_D}{100}\right)^2 \times \frac{T}{365} \equiv 2e^{rT} \sum_{j=1}^N \frac{\Delta K_j}{K_j^2} P_0(K_j) \rightarrow CIV^D \quad (14)$$

However, due to the correction term in the computation of the CBOE VIX as in Equation (1), the sum of VIX_U^2 and VIX_D^2 is not exactly equal to VIX^2 , and we instead use \widetilde{VIX}_U^2 and \widetilde{VIX}_D^2 obtained from the following scaling procedure:

$$\widetilde{VIX}_U^2 = VIX^2 \times \frac{VIX_U^2}{VIX_U^2 + VIX_D^2} \quad (15)$$

$$\widetilde{VIX}_D^2 = VIX^2 \times \frac{VIX_D^2}{VIX_U^2 + VIX_D^2} \quad (16)$$

4 Model-Implied Pricing Formulas

4.1 VIX Pricing Formula

For a model with Gaussian innovations to daily log returns, one could directly use the formula (6) to derive the model-implied VIX index, as it can be interpreted as measuring the risk-neutral expectation of integrated variance. This is not the case for a model with jumps or nonnormality, and we need to use the original formula in Equation (3). Thus, for the GSARV model, we have the following pricing formula for the VIX index:

Proposition 1. *If the return of the S&P 500 index follows the GSARV model, then the model-implied 1-month ahead VIX can be expressed as*

$$VIX_t = 100\sqrt{252} \times \sqrt{-2(\bar{r}^* - r) + 2\xi_u^* V_{u,t}(22) + 2\xi_d^* V_{d,t}(22)}$$

where $V_{u,t}(n)$ and $V_{d,t}(n)$ are the average expected upside/downside volatility over the next

⁷We follow the same interpolation methodology used in CBOE to calculate VIX_U^2 and VIX_D^2 for a specific maturity T , i.e., 30 calendar days.

n trading days in risk-neutral measure \mathbb{Q} , given by:

$$V_{j,t}(n) \equiv \frac{1}{n} \sum_{i=1}^n \mathbb{E}_t^{\mathbb{Q}} (h_{j,t+i}^*) = (1 - \Gamma_j(n)) \bar{h}_j^* + \Gamma_j(n) h_{j,t+1}^*, \quad j = \{u, d\}$$

with

$$\Gamma_j(n) = \frac{1 - (\beta_j + \alpha_j^* \gamma_j^{*2})^n}{n \left[1 - (\beta_j + \alpha_j^* \gamma_j^{*2}) \right]}, \quad \bar{h}_j^* = \frac{\omega_j^* + \alpha_j^*}{1 - (\beta_j + \alpha_j^* \gamma_j^{*2})} + \omega_j^*$$

Proof: see Appendix B.

Proposition 1 shows that the VIX pricing formula of GSARV is a combination of risk-neutral expectations of future upward and downward volatility, and the weights are adjusted based on the nonnormality of the type of each shock. In fact, when $\omega_j^* \rightarrow 0$, i.e. $z_{j,t}^* \xrightarrow{d} N(0, h_{j,t}^*)$, we have $\bar{r}^* \rightarrow r_f$ and $\xi_j^* \rightarrow \frac{1}{2}$, then the VIX approaches the expectation of integrated variance shown in Equation (6).

4.2 Risk-Neutral Semivariance Pricing Formula

This section shows how to derive the model-implied risk-neutral semivariance. Recall that when F_t follows a diffusion process in Equation (4), we have the pricing formula for the VIX defined on the dynamics of the volatility process using Equation (6). In the discrete-time setting, we can calculate the VIX as the expected arithmetic average of the variance over the next 22 trading days. The implementation is simple because the model-implied expected variance is always analytical. When it comes to the risk-neutral semivariance CIV_T^U and CIV_T^D expressed in Equation (11) and (12), things become complicated as it is not straightforward to compute the conditional expectation of $\sigma_t^2 \mathbb{I}_{\{F_t \leq F_0\}}$. Therefore, we resort to Equation (9) and (10) to derive our model-implied risk-neutral semivariance.

Proposition 2. *Under the definitions in Equations (9) and (10), the model-implied risk-neutral upside/downside variance can be expressed as*

$$\begin{aligned} \text{CIV}_t^U &= \frac{2}{\pi} \int_0^\infty \Re \left[e^{-ur(T-t)} \left(\frac{1}{u-1} - \frac{1}{u} - \frac{1}{u^2} \right) \phi_t(u, T) \right] du_I \\ \text{CIV}_t^D &= \frac{2}{\pi} \int_0^\infty \Re \left[e^{-vr(T-t)} \left(\frac{1}{1-v} + \frac{1}{v} + \frac{1}{v^2} \right) \phi_t(v, T) \right] dv_I \end{aligned}$$

where u, v are two complex numbers denoted by $u = u_R + iu_I$ and $v = v_R + iv_I$, with $u_R > 1$, $v_R < 0$, and $u_I, v_I \in \mathbb{R}$. The operator $\Re[\cdot]$ takes the real part of the complex number in the square brackets. Function $\phi_t(s, T)$ is the characteristic function of future cumulative

returns, defined as

$$\phi_t(s, T) = \mathbb{E}_t^{\mathbb{Q}} \left[\exp \left(s \sum_{i=1}^{T-t} R_{t+i} \right) \right], \quad R_\tau = \log(S_\tau/S_{\tau-1})$$

Proof: see Appendix C.

Note that the pricing formulas of CIV_t^U and CIV_t^D provided in Proposition 2 are not restricted to a specific model. It is possible to derive the model-implied risk-neutral upside/downside variance using these formulas if the closed-form expression of the characteristic function of future cumulative returns is available. For the GSARV model, according to Feunou & Okou (2019, Appendix A), $\phi_t(s, T)$ is given by

$$\phi_t(s, T) = \exp \left(D(s, T-t) + C_u(s, T-t)h_{u,t+1}^* + C_d(s, T-t)h_{d,t+1}^* \right)$$

where $D(s, M)$, $C_u(s, M)$, and $C_d(s, M)$ can be obtained by an iterative relationship.

4.3 Model-Implied VIX Futures Pricing Formula

In this section, we investigate the VIX futures pricing performance of the GSARV model. Following Zhu & Lian (2012, Proposition 1), the VIX futures price at time t with maturity date T can be presented as the conditional expectation of the VIX under the risk-neutral measure, i.e., $F(t, T) = \mathbb{E}_t^{\mathbb{Q}}(\text{VIX}_T)$. Proposition 3 presents the GSARV model-implied VIX futures prices.

Note that it is possible to extend our work to VIX option pricing, as the GSARV model is an affine model with an analytical moment generating function (MGF) for future conditional variance (see Appendix D), which is the key to derive the VIX option pricing formula (Cao et al., 2020; Tong & Huang, 2021). However, a rigorous analysis of the VIX option pricing performance of the GSARV model would be a stupendous feat and is not the main goal of this paper. Therefore, we leave it for future research.

Proposition 3. *If the return of the S&P 500 index follows the GSARV model, then the model-implied VIX futures price can be expressed as*

$$F(t, T) = \frac{50\sqrt{252}}{\sqrt{\pi}} \int_0^\infty \frac{1 - e^{2v(\bar{r}^* - r)} \Psi_{u,t}(-2v\xi_u^*, T) \Psi_{d,t}(-2v\xi_d^*, T)}{v^{3/2}} dv$$

where $\Psi_{j,t}(s, T)$, $j = \{u, d\}$ is the conditional MGF of $V_{j,T}(22)$, given by

$$\Psi_{j,t}(s, T) = \mathbb{E}_t^{\mathbb{Q}} \left[\exp(sV_{j,T}(22)) \right] = \exp \left(H_j(s, T-t) + G_j(s, T-t)h_{j,t+1}^* \right)$$

where $H_j(s, m)$, $G_j(s, m)$ can be obtained by the following iterative relationship:

$$\begin{aligned} H_j(s, m+1) &= H_j(s, m) + G_j(s, m) (\omega_j^* + \bar{\omega}_j^* - \omega_j^* \beta_j) \\ &\quad - \frac{\omega_j^* \alpha_j^* \gamma_j^{*2} G_j(s, m)}{1 - 2\alpha_j^* G_j(s, m)} - \frac{1}{2} \log(1 - 2\alpha_j^* G_j(s, m)) \\ G_j(s, m+1) &= \frac{\alpha_j^* \gamma_j^{*2} G_j(s, m)}{1 - 2\alpha_j^* G_j(s, m)} + \beta_j G_j(s, m) \end{aligned}$$

with initial conditions

$$H_j(s, 0) = s(1 - \Gamma_j(22)) \bar{h}_j^*, \quad G_j(s, 0) = s\Gamma_j(22)$$

Proof: see Appendix D.

5 Competing Models

5.1 Affine Realized Variance (ARV) Model

Similar to [Feunou & Okou \(2019\)](#), we focus on a restricted version of the GSARV model by fixing $\omega \equiv \omega_u = \omega_d = 0$ and $h_{u,t} = h_{d,t}$, by which we obtain

$$\begin{aligned} R_{t+1} &= r + \left(\lambda - \frac{1}{2}\right) h_{t+1} + \sqrt{h_t} \varepsilon_{t+1} \\ h_{t+1} &= \bar{\omega} + \beta h_t + \alpha \left(v_t - \gamma \sqrt{h_t}\right)^2 \\ RV_t &= h_t + \sigma \left[\left(v_t - \gamma \sqrt{h_t}\right)^2 - 1 - \gamma^2 h_t \right] \end{aligned}$$

The innovations (ε_t, v_t) follow a standard bivariate normal distribution with the correlation of ρ . This single-factor specification is identical to the affine realized variance (ARV) model of [Christoffersen et al. \(2014\)](#). Its risk-neutralization process can be simply adapted from the GSARV model.

5.2 Heston-Nandi GARCH (HN-GARCH) Model

As a widely cited benchmark option pricing model, the Heston-Nandi GARCH (HN-GARCH) model proposed by [Heston & Nandi \(2000\)](#) is one of the very few discrete-time volatility models that yield an analytical MGF for cumulative returns. The physical dy-

namics of the HN-GARCH model are given by

$$\begin{aligned} R_{t+1} &= r + (\lambda - \frac{1}{2})h_{t+1} + \sqrt{h_{t+1}}z_{t+1}, \quad z_{t+1} \stackrel{\text{iid}}{\sim} \text{N}(0, 1) \\ h_{t+1} &= \omega + \beta h_t + \alpha \left(z_t - \gamma \sqrt{h_t} \right)^2. \end{aligned}$$

The corresponding risk-neutral dynamics with the variance-augmented pricing kernel of [Christoffersen et al. \(2013\)](#) are given by

$$\begin{aligned} R_{t+1} &= r - \frac{1}{2}h_{t+1}^* + \sqrt{h_{t+1}^*}z_{t+1}^*, \quad z_{t+1}^* \stackrel{\text{iid}}{\sim} \text{N}(0, 1) \\ h_{t+1}^* &= \omega^* + \beta h_t^* + \alpha^* \left(z_t^* - \gamma^* \sqrt{h_t^*} \right)^2, \end{aligned}$$

The model-implied MGF of future cumulative returns can be found in [Christoffersen et al. \(2013\)](#) and its VIX futures pricing formula is provided in [Wang et al. \(2017\)](#).

5.3 Inverse-Gaussian GARCH (IG-GARCH) Model

As an extension to the HN-GARCH model, [Christoffersen et al. \(2006\)](#) proposed the Inverse-Gaussian GARCH (IG-GARCH) model to allow for the conditional skewness of future returns. As we are interested in models with asymmetry of distribution, we adopt this model as another benchmark. The IG-GARCH model is given by

$$\begin{aligned} R_{t+1} &= r + \xi h_{t+1} + \eta \varepsilon_{t+1}, \quad \varepsilon_{t+1} \sim \text{IG}(h_{t+1}/\eta^2) \\ h_{t+1} &= \omega + \beta h_t + \gamma \varepsilon_t + \frac{\alpha h_t^2}{\varepsilon_t} \end{aligned}$$

where the shock ε_{t+1} follows an inverse Gaussian distribution with the degree of freedom $\frac{h_{t+1}}{\eta^2}$. Following [Cao et al. \(2020\)](#), we use a two-dimensional pricing kernel to obtain the risk-neutral process

$$\begin{aligned} R_{t+1} &= r + \xi^* h_{t+1}^* + \eta^* \varepsilon_{t+1}^*, \quad \varepsilon_{t+1}^* \sim \text{IG}(h_{t+1}^*/\eta^{*2}) \\ h_{t+1}^* &= \omega^* + \beta h_t^* + \gamma^* \varepsilon_t^* + \frac{\alpha^* h_t^{*2}}{\varepsilon_t^*} \end{aligned}$$

The model-implied MGF of future cumulative returns and the VIX futures pricing formula can be found in [Christoffersen et al. \(2006\)](#) and [Yang & Wang \(2018\)](#), respectively.

6 Parameter Calibration

In our paper, as we decompose the market VIX into its upside and downside components, which are all observable to us now, we directly calibrate the model's risk-neutral parameters by matching the model-implied risk-neutral semivariance (VIX_U^m and VIX_D^m) with the corresponding observed market indexes (VIX_U and VIX_D). Specifically, the pricing error is assumed to follow a bivariate normal distribution

$$e_t^{\text{VIX}} = \begin{pmatrix} e_{u,t} \\ e_{d,t} \end{pmatrix} = \begin{pmatrix} VIX_{U,t} - VIX_{U,t}^m \\ VIX_{D,t} - VIX_{D,t}^m \end{pmatrix} \stackrel{\text{iid}}{\sim} N \left[\begin{pmatrix} 0 \\ 0 \end{pmatrix}, \begin{pmatrix} \sigma_u^2 & 0 \\ 0 & \sigma_d^2 \end{pmatrix} \right]$$

We assume that the pricing errors for different VIX components are independent, so the sample log-likelihood function can be decomposed as follows:

$$\ell_{\text{VIX}} = \underbrace{-\frac{1}{2} \sum_{t=1}^T \left\{ \log(2\pi\sigma_u^2) + \frac{e_{u,t}^2}{\sigma_u^2} \right\}}_{\ell_{\text{VIX}^U}} + \underbrace{-\frac{1}{2} \sum_{t=1}^T \left\{ \log(2\pi\sigma_d^2) + \frac{e_{d,t}^2}{\sigma_d^2} \right\}}_{\ell_{\text{VIX}^D}}$$

where T is the number of trading days, and σ_u^2 and σ_d^2 can be estimated with the sample variance of pricing errors according to the first-order conditions to maximize the log-likelihood function. In our empirical analysis, for the pricing of the VIX index and its upside/downside components, we calibrate the model parameters by maximizing ℓ_{VIX} .

In this paper, we also focus on the pricing of the panel of VIX futures. Following [Huang et al. \(2019\)](#), we assume that the pricing errors are independently and normally distributed with zero mean and constant variance σ_{Fut}^2 ; the sample log-likelihood function is given by

$$\ell_{\text{Fut}} = -\frac{1}{2} \sum_{i=1}^N \left\{ \log(2\pi\sigma_{\text{Fut}}^2) + \frac{e_{i,t}^2}{\sigma_{\text{Fut}}^2} \right\}$$

where N is the number of total VIX futures prices. This sample log-likelihood function is used to calibrate the parameters used for pricing VIX futures.

7 Empirical Results

7.1 Data

We collect data on daily S&P 500 index return, realized semivariance, and the CBOE VIX index. We construct the daily upside and downside VIX indexes using OTM SPX option

prices based on formulas (13) to (16). To overcome the possible microstructure noise problem, the realized variance is calculated using 5-minute returns, as well as the realized semivariance. In line with Feunou & Okou (2019), these realized measures of volatility are re-scaled to match the sample variance of daily close-to-close returns.

We also collect the panel of VIX futures prices.⁸ The VIX futures data start in March 2004, so our full sample spans approximately 17 years from March 31, 2004 to December 31, 2020. Following Zhu & Lian (2012), several filters are applied. First, VIX futures with less than 5 days to maturity are removed. Second, futures with an open interest of less than 200 contracts are excluded to avoid any liquidity-related bias. Finally, we keep all VIX futures with a time to maturity of up to 90 days.⁹ The sample includes 4,241 daily observations for the underlying data and 11,376 observations for VIX futures prices.

Table 1 reports the summary statistics of our data set. Panel A is for the time series data. The S&P 500 returns exhibit a small negative skewness and a high level of kurtosis. The realized variance and the VIX are both positively skewed and leptokurtic. The sample mean of the realized variance is 15.145%, substantially smaller than the average VIX at 18.897%. Their difference reflects the (average) negative volatility risk premium. The upside and downside realized semivariances have similar magnitudes. However, when it comes to risk-neutral measures, sizable discrepancies arise for the upside and downside components of the VIX. We find that compared with the upside VIX, the downside part is much larger with a higher standard deviation. An interesting finding is that the sample mean of the upside (downside) component of the VIX is smaller (larger) than the realized upside (downside) variance, which means that there exists an average negative (positive) premium on the upside (downside) variance.

Figure 1 plots the time series of the upside and downside components of the VIX from January 1, 1996 to December 31, 2020.¹⁰ These two time series exhibit markedly higher persistence, dispersion, positive asymmetry, and heavy tail than the distribution of returns. In line with our findings in the summary statistics, the downside components are larger than the upside part. For the VIX futures data in Panel B of Table 1, we find that (a) the average prices are higher in longer maturities; (b) the standard deviation of futures prices decreases almost monotonically with maturity; and (c) the average prices are much higher when the level of basis (VIX level minus VIX futures price) increases; and (d) the VIX futures market is always in contango as the basis is negative most of the time.

⁸We obtain the daily S&P 500 index from Yahoo Finance. The realized measures are collected from the Realized Library of the Oxford-Man Institute, and the VIX index and VIX futures are from CBOE's website.

⁹In our dataset, VIX futures with maturities of less than 90 days account for 89.1% of total trading volume.

¹⁰The SPX option prices used to construct the upside/downside components of the VIX are provided by WRDS OptionMetrics; these are available from January 1996 onward.

Table 1: Summary Statistics

	Mean(%)	Std(%)	Skew	Kurt	Obs.
<i>Panel A: S&P 500 returns, Realized Measures of Volatility, and CBOE VIX</i>					
Returns (annualized)	7.973	19.416	-0.563	17.355	4,241
Realized Variance (RV)	15.145	12.152	3.700	24.570	4,241
Upside RV	10.569	8.627	3.839	26.519	4,241
Downside RV	10.431	9.075	3.735	24.577	4,241
VIX	18.897	9.261	2.581	12.067	4,241
Upside VIX	10.214	5.178	2.561	12.110	4,241
Downside VIX	15.873	7.730	2.581	12.079	4,241
<i>Panel B: CBOE VIX Futures</i>					
All VIX Futures	20.335	7.705	1.856	7.543	11,376
<i>Partitioned by VIX level</i>					
VIX < 15	14.702	1.751	0.256	3.162	4,681
15 ≤ VIX < 30	21.715	4.304	0.563	2.426	5,613
30 ≤ VIX	37.547	8.454	0.804	3.499	1,082
<i>Partitioned by days to maturity</i>					
DTM < 30	19.573	8.400	2.205	9.178	3,779
30 ≤ DTM < 60	20.363	7.435	1.691	6.336	3,701
60 ≤ DTM	21.048	7.166	1.613	6.310	3,896
<i>Partitioned by basis level</i>					
Basis < -2	19.761	5.735	1.239	5.202	4,388
-2 ≤ Basis < 0	18.281	6.263	1.815	6.893	4,776
0 ≤ Basis	25.910	10.706	1.225	4.075	2,212

Note: Summary statistics for close-to-close S&P 500 index log returns, upside/downside realized measures of volatility (in square root form), CBOE VIX, upside/downside VIX, and VIX futures prices from March 31, 2004, to December 31, 2020. The reported statistics include the sample mean (Mean), standard deviation (Std), skewness (Skew), kurtosis (Kurt), and number of observations (Obs). DTM denotes the number of calendar days to maturity. Basis = VIX level minus VIX futures price. Data sources: S&P 500 returns from WRDS; VIX index and VIX futures from the CBOE website; realized measures from the Realized Library of Oxford-Man Institute; upside/downside VIX computed using SPX option prices from WRDS OptionMetrics.

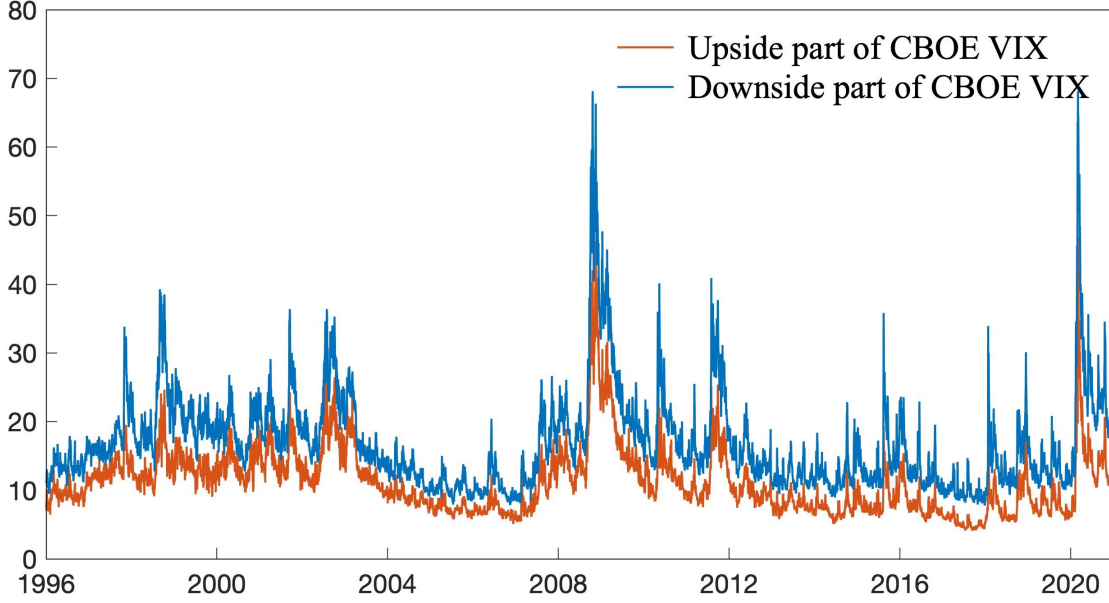


Figure 1: This figure shows the time series data of the upside and downside components of the CBOE VIX from January 1, 1996 to December 31, 2020. The CBOE VIX index is decomposed based on the formulas (13) to (16) using OTM SPX options from WRDS OptionMetrics.

7.2 Pricing VIX and its Upside/Downside Components

Table 2 presents the in-sample parameter calibration results for each model from March 2004 to December 2020 using VIX components. The estimated risk-neutral parameters, robust standard errors, persistence of volatility dynamics, and log-likelihood are all reported. Note that to make a concise table, for one-factor models, the reported parameter, e.g. β_u , is actually the parameter β . Several results can be observed. First, as indicated by $\pi^{\mathbb{Q}}$, most models have a highly persistent volatility process under risk-neutral measures. Second, for the IG-GARCH model, the parameter η^* that generates conditional skewness is negative and significant¹¹.

The results for the GSARV model are quite interesting. First, shifting ARV to the GASRV model does improve the empirical fit of the model, as illustrated by the increased value of the log-likelihood functions. Second, although the sample means of the upside/downside variance in the physical measure are similar, their magnitude in risk-neutral measure are markedly higher, as indicated by \bar{h}_u^* and \bar{h}_d^* . Third, from VRP_u and VRP_d , we do find a negative (positive) premium on the upside (downside) variance. This means that investors show asymmetric behavior toward good versus bad uncertainty: they like good uncertainty but dislike bad uncertainty. This result is also consistent with the finding of

¹¹When η^* goes to zero, the inverse-gaussian distribution will converge to a normal distribution.

Feunou et al. (2017). Fourth, the parameter α_d^* is much larger than α_u^* , which means that the realized downside variance is more informative than its upside counterpart. Finally, the correlations between return shocks and realized variance are much stronger for the downside part than for the upside part. In other words, the parameters controlling the dynamics for upside and downside volatility show sizable differences. This means that it is important to allow for distinct upside/downside variance dynamics.

In Table 3, we report the in-sample performance of pricing the VIX and its components. We compare the model-based price, P_t^m , with the market-observed price, P_t . The resulting full-sample root of mean square error (RMSE),

$$\text{RMSE} = \sqrt{\frac{1}{T} \sum_{t=1}^T (P_t - P_t^m)^2}, \quad P_t \in \{\text{VIX}_t, \text{VIX}_{U,t}, \text{VIX}_{D,t}\}$$

is reported in the first row of Table 3. For the IG-GARCH, ARV, and GSARV models, we report the ratios of their RMSEs to the benchmark HN-GARCH model. Therefore, a ratio less than one indicates better pricing performance relative to the HN-GARCH model.

In terms of overall performance, the models with realized measures (ARV/GASRV) generally perform better than those based solely on daily returns (HN/IG-GARCH), with a reduction in RMSE from 20.6% to 39.6%. Among these models, the GSARV model has the best fit. The GARCH model with conditional skewness performance is better than the HN-GARCH model, but the improvement is relatively small. When we compare the pricing performance of different VIX components, the findings are quite interesting. First, we find that the improvement of the ARV model is more significant in pricing the downside component of the VIX than its upside counterpart. Recall that the ARV model only uses the unsigned realized variance; therefore, these results mean that this conventional realized variance does not provide enough information for the upside part of the implied variance. Second, when it comes to the GSARV model, the improvements in the upside/downside components of the VIX index are more balanced and larger. These results provide strong evidence that the spread between upside/downside variance is the main driver of asymmetry in stock price distributions.

7.3 Pricing VIX Futures

Table 4 presents the in-sample parameter calibration results from March 2004 to December 2020 using VIX futures prices. The main findings regarding the estimated parameters are similar to those of Table 2, and we do not discuss them further here. Note that when fitting the VIX futures prices, the correlations between return shocks and realized measures, i.e.

Table 2: Estimation Results Using VIX Components (2004-2020)

	HN-GARCH	IG-GARCH	ARV	GSARV
β_u	0.620 (0.001)	-5.683 (0.196)	0.934 (0.048)	0.999 (0.069)
α_u^*	2.90E-06 (1.48E-09)	1.90E+06 (3.64E+05)	4.22E-08 (5.75E-09)	1.36E-11 (2.72E-12)
γ_u^*	3.56E+02 (0.77)	5.48E-06 (2.89E-07)	1.20E+03 (3.67E-01)	1.22E+02 (4.97E-01)
σ_u^*			6.39E-07 (9.00E-08)	1.36E-09 (8.67E-08)
ρ_u^*			0.442 (0.022)	0.408 (0.023)
ζ_u^*			4.56E-05 (9.67E-06)	-7.83E-06 (5.37E-07)
ϕ_u^*			0.874 (0.122)	0.756 (0.188)
ω_u^*				3.04E-08 (5.49E-09)
β_d				0.973 (0.089)
α_d^*				5.35E-08 (7.93E-09)
γ_d^*				7.08E+02 (5.33E+01)
σ_d^*				3.30E-07 (6.74E-08)
ρ_d^*				0.922 (0.013)
ζ_d^*				3.84E-05 (3.87E-06)
ϕ_d^*				1.199 (0.440)
ω_d^*				1.47E-05 (3.47E-06)
η^*		-1.14E-03 (1.94E-05)		
\bar{h}_u^* \bar{h}_d^*	2.49E-04	2.51E-04	1.83E-04	5.09E-05 1.34E-04
$\pi_u^{\mathbb{Q}}$ $\pi_d^{\mathbb{Q}}$	0.988	0.988	0.999	0.999 0.999
VRP _u VRP _d			2.58E-05	-2.66E-05 5.41E-05
$\ell_{\text{vix}U}$	-12492	-12359	-11611	-10338
$\ell_{\text{vix}D}$	-14625	-14536	-12967	-11938
ℓ_{vix}	-27117	-26895	-24578	-22276

Note: Estimation results for the full sample period (March 31, 2004 to December 31, 2020) using VIX components. The estimated parameters are reported with robust standard errors (in parentheses), $\pi^{\mathbb{Q}}$ refers to volatility persistence under \mathbb{Q} . The value of the log-likelihood function is reported at the bottom of the table.

Table 3: In-Sample VIX Pricing Performance (2004 - 2020)

Model	RMSE		Ratio to HN-GARCH	
	HN-GARCH	IG-GARCH	ARV	GSARV
CBOE VIX	4.106	0.988	0.804	0.604
<i>Partitioned by VIX components</i>				
Upside VIX	2.455	0.980	0.822	0.599
Downside VIX	3.929	0.994	0.702	0.595

Note: This table reports the in-sample pricing performance of each model for the VIX (and its upside/downside components) from March 31, 2004 to December 31, 2020. We evaluate the model’s pricing ability through the RMSE. For the IG-GARCH, ARV, and GSARV models, we report the ratios of their RMSEs to the benchmark HN-GARCH model.

the parameters ρ_u^* and ρ_d^* , are unidentified, as the distribution of returns is not involved explicitly in the dynamics of the two variances.

In Table 5, we report the in-sample VIX futures pricing performances. We compare the model-based price, F_i^m , with the market-observed price, F_i . The full-sample RMSE,

$$\text{RMSE} = \sqrt{\frac{1}{N} \sum_{i=1}^N (F_i - F_i^m)^2},$$

is reported in the first row of Table 5. As in Table 3, for the IG-GARCH, ARV, and GSARV models, we report the ratios of their RMSEs to the HN-GARCH model.

Table 5 presents the RMSE for VIX futures where the model parameters are given in Table 4. In addition, the total RMSE for VIX futures pricing is decomposed by VIX level, time to maturity, and basis of futures prices. The first dimension is linked to the volatility level of the market. The second is linked to the model’s ability to track volatility dynamics at different time horizons, and the last allows us to check the model’s performance under different market conditions. We find that the models with realized measures still perform better. Among these models, the GSARV model has the best fit, with a reduction in RMSE of up to 23.4%. The HN-GARCH and IG-GARCH models are the two models without realized measures. The nonnormality structure of IG-GARCH enables it to perform better than the HN-GARCH model in periods with low VIX levels or in the deep contango market. It is interesting to compare the ARV model and the GARV model, as the former is a special case of the GARV model without splitting realized variance. The improvements resulting

Table 4: Estimation Results Using VIX Futures (2004-2020)

	HN-GARCH	IG-GARCH	ARV	GSARV
β_u	0.792 (0.002)	-4.938 (0.191)	0.995 (0.014)	0.999 (0.040)
α_u^*	1.06E-06 (8.39E-08)	4.59E+06 (2.72E+05)	3.48E-11 (1.45E-09)	2.09E-09 (3.49E-12)
γ_u^*	4.40E+02 (0.09)	1.84E-06 (1.67E-07)	8.07E+01 (9.67E-01)	1.42E+02 (8.87E-01)
σ_u^*			2.90E-07 (9.67E-08)	3.49E-09 (7.67E-10)
ζ_u^*			-5.08E-05 (9.67E-06)	-2.52E-05 (7.37E-06)
ϕ_u^*			1.547 (0.122)	1.025 (0.218)
ω_u^*				2.12E-09 (7.37E-10)
β_d				0.987 (0.078)
α_d^*				1.45E-08 (4.36E-09)
γ_d^*				6.80E+01 (4.33E-01)
σ_d^*				3.63E-07 (3.78E-08)
ζ_d^*				-8.67E-06 (1.37E-06)
ϕ_d^*				1.843 (0.423)
ω_d^*				5.75E-06 (2.97E-07)
η^*		-7.17E-04 (2.17E-05)		
\bar{h}_u^*	3.99E-04	4.14E-04	1.93E-04	5.44E-05
\bar{h}_d^*				1.38E-04
$\pi_u^{\mathbb{Q}}$	0.997	0.997	0.995	0.999
$\pi_d^{\mathbb{Q}}$				0.987
VRP _u			3.51E-05	-2.33E-05
VRP _d				5.82E-05
ℓ_{Fut}	-29017	-28687	-28120	-26095

Note: Estimation results for the full sample period (March 31, 2004 to December 31, 2020) using VIX futures prices. The estimated parameters are reported with robust standard errors (in parentheses), $\pi^{\mathbb{Q}}$ refers to volatility persistence under \mathbb{Q} . The value of the log-likelihood function is reported at the bottom of the table.

Table 5: In-Sample VIX Futures Pricing Performance (2004 - 2020)

Model	RMSE	Ratio to HN-GARCH		
	HN-GARCH	IG-GARCH	ARV	GSARV
Full-sample	3.101	0.971	0.924	0.766
<i>Panel A: Partitioned by VIX level</i>				
VIX < 15	2.097	0.911	0.806	0.627
15 ≤ VIX < 30	2.752	0.962	1.006	0.854
30 ≤ VIX	6.543	1.006	0.895	0.735
<i>Panel B: Partitioned by days to maturity</i>				
DTM < 30	3.528	0.984	0.897	0.680
30 ≤ DTM < 60	2.833	0.961	0.929	0.830
60 ≤ DTM	2.895	0.963	0.958	0.819
<i>Panel C: Partitioned by basis level</i>				
Basis < -2	2.460	0.959	1.035	0.878
-2 ≤ Basis < 0	2.685	0.951	0.902	0.720
0 ≤ Basis	4.679	0.992	0.874	0.729

Note: This table reports the in-sample VIX futures pricing performance of each model from March 31, 2004 to December 31, 2020. We evaluate the model's pricing ability through the RMSE. For the IG-GARCH, ARV, and GSARV models, we report the ratios of their RMSEs to the benchmark HN-GARCH model. We summarize the results by VIX level, Basis (VIX level minus VIX futures price), and days to maturity. DTM denotes the number of calendar days to maturity.

Table 6: Out-of-Sample VIX Pricing Performance (2009 - 2020)

Model	RMSE	Ratio to HN-GARCH		
	HN-GARCH	IG-GARCH	ARV	GSARV
CBOE VIX	4.591	0.976	0.762	0.574
<i>Partitioned by VIX components</i>				
Upside VIX	2.578	0.982	0.840	0.608
Downside VIX	4.423	0.976	0.685	0.559

Note: This table reports the out-of-sample VIX futures pricing performance of each model from April 1, 2009 to December 31, 2020. The out-of-sample performance evaluation is based on a rolling window of 1,000 trading days, with the parameters updated on a monthly basis. We evaluate the model’s pricing ability through the RMSE. For the IG-GARCH, ARV, and GSARV models, we report the ratios of their RMSEs to the benchmark HN-GARCH model. We summarize the results by VIX level, Basis (VIX level minus VIX futures price), and days to maturity. DTM denotes the number of calendar days to maturity.

from the use of unsigned realized variance are concentrated in cases where the VIX level is extremely high/low, VIX futures are short term, and the market is in backwardation. The GSARV model based on signed semivariance outperforms the ARV model in every subcategory, especially in low-volatility market conditions, when the upside component contains rich information about the underlying process.

7.4 Out-of-Sample Pricing Performance

When considering models with realized measures, the number of parameters increases for the ARV and GSARV models. It is important to check if the superior performance of these models does not merely result from in-sample overfitting. As in [Huang et al. \(2019\)](#), we conduct an out-of-sample pricing analysis based on a rolling window of 1,000 trading days, with the parameters updated on a monthly basis. We evaluate the out-of-sample pricing errors from April 1, 2009 to December 31, 2020 (the observations in the first 5 years are used as a presample to obtain the first set of parameters).

In [Tables 6 and 7](#), we report the out-of-sample VIX and VIX futures pricing performance results, respectively. We find that the results are very similar to those reported in [Tables 3 and 5](#). The GSARV model still generates the smallest pricing error, and the main findings remain. Based on these results, we can conclude that the improvements resulting from splitting realized variance are not caused by in-sample overfitting.

Table 7: Out-of-Sample VIX Futures Pricing Performance (2009 - 2020)

Model	RMSE	Ratio to HN-GARCH		
	HN-GARCH	IG-GARCH	ARV	GSARV
Full-sample	2.928	0.978	0.948	0.799
<i>Panel A: Partitioned by VIX level</i>				
VIX < 15	2.554	0.936	0.800	0.737
15 ≤ VIX < 30	3.040	0.992	1.039	0.867
30 ≤ VIX	3.826	1.003	0.809	0.563
<i>Panel B: Partitioned by days to maturity</i>				
DTM < 30	3.272	0.991	0.940	0.765
30 ≤ DTM < 60	2.702	0.969	0.942	0.827
60 ≤ DTM	2.794	0.968	0.963	0.816
<i>Panel C: Partitioned by basis level</i>				
Basis < -2	3.552	0.982	1.004	0.840
-2 ≤ Basis < 0	2.327	0.963	0.651	0.614
0 ≤ Basis	2.031	0.968	0.843	0.705

Note: This table reports the out-of-sample VIX futures pricing performance of each model from April 1, 2009 to December 31, 2020. The out-of-sample performance evaluation is based on a rolling window of 1000 trading days, with the parameters updated on a monthly basis. We evaluate the model's pricing ability through the RMSE. For the IG-GARCH, ARV, and GSARV models, we report the ratios of their RMSEs to the benchmark HN-GARCH model. We summarize the results by the VIX level, Basis (VIX level-VIX futures price), and days to maturity. DTM denotes the number of calendar days to maturity.

8 Conclusion

This paper investigates the role of realized semivariance in pricing the CBOE VIX and VIX futures, using the GSARV model of [Feunou & Okou \(2019\)](#). We obtain the closed-form pricing formula for both the VIX and VIX futures, and show that the new model provides superior pricing performance, both in-sample and out-of-sample. We further analytically derive the pricing formulas for the upside/downside components of the VIX. Such decomposition shows that the information gains from the conventional realized variance are more significant on pricing the downside component of the VIX, while the new model incorporating signed realized semivariance provides a larger and balanced improvement in both upside/downside components of the VIX. Our results provide strong evidence supporting the spread between upside/downside variance as the main driver of asymmetry in stock price distributions.

References

- Andersen, T. G. & Bondarenko, O. (2007). Construction and interpretation of model-free implied volatility. In *Volatility As An Asset Class* (pp. 141–181). Risk Publications.
- Andersen, T. G., Bondarenko, O., & Gonzalez-Perez, M. T. (2015). Exploring return dynamics via corridor implied volatility. *The Review of Financial Studies*, 28(10), 2902–2945.
- Bakshi, G. & Madan, D. (2000). Spanning and derivative-security valuation. *Journal of Financial Economics*, 55(2), 205–238.
- Barndorff-Nielsen, O. E., Kinnebrock, S., & Shephard, N. (2010). Measuring downside risk–realised semivariance. In M. W. Watson, T. Bollerslev, & J. Russell (Eds.), *Volatility and Time Series Econometrics: Essays in Honor of Robert Engle* (pp. 117–137). Oxford University Press.
- Britten-Jones, M. & Neuberger, A. (2000). Option prices, implied price processes, and stochastic volatility. *Journal of Finance*, 55(2), 839–866.
- Cao, H., Badescu, A., Cui, Z., & Jayaraman, S. K. (2020). Valuation of VIX and target volatility options with affine GARCH models. *Journal of Futures Markets*, 40(12), 1880–1917.
- Carr, P. & Madan, D. (2001). Optimal positioning in derivative securities. *Quantitative Finance*, 1(1), 19–37.

- Christoffersen, P., Feunou, B., Jacobs, K., & Meddahi, N. (2014). The economic value of realized volatility: Using high-frequency returns for option valuation. *Journal of Financial and Quantitative Analysis*, 49(3), 663–697.
- Christoffersen, P., Heston, S., & Jacobs, K. (2006). Option valuation with conditional skewness. *Journal of Econometrics*, 131(1), 253–284.
- Christoffersen, P., Heston, S., & Jacobs, K. (2013). Capturing option anomalies with a variance-dependent pricing kernel. *Review of Financial Studies*, 26(8), 1963–2006.
- Corsi, F., Fusari, N., & Vecchia, D. L. (2013). Realizing smiles: Options pricing with realized volatility. *Journal of Financial Economics*, 107, 284–304.
- Dotsis, G. & Vlastakis, N. (2016). Corridor volatility risk and expected returns. *Journal of Futures Markets*, 36(5), 488–505.
- Engle, R. F. & Gallo, G. M. (2006). A multiple indicators model for volatility using intra-daily data. *Journal of Econometrics*, 131(1-2), 3–27.
- Feunou, B., Jahan-Parvar, M. R., & Okou, C. (2017). Downside variance risk premium. *Journal of Financial Econometrics*, 16(3), 341–383.
- Feunou, B., Jahan-Parvar, M. R., & Tédongap, R. (2011). Modeling market downside volatility. *Review of Finance*, 17(1), 443–481.
- Feunou, B., Jahan-Parvar, M. R., & Tédongap, R. (2016). Which parametric model for conditional skewness? *The European Journal of Finance*, 22(13), 1237–1271.
- Feunou, B. & Okou, C. (2019). Good volatility, bad volatility, and option pricing. *Journal of Financial and Quantitative Analysis*, 54(2), 695–727.
- Fu, X., Sandri, M., & Shackleton, M. B. (2016). Asymmetric effects of volatility risk on stock returns: Evidence from VIX and VIX futures. *Journal of Futures Markets*, 36(11), 1029–1056.
- Hansen, P. R. & Huang, Z. (2016). Exponential GARCH modeling with realized measures of volatility. *Journal of Business & Economic Statistics*, 34(2), 269–287.
- Hansen, P. R., Huang, Z., & Shek, H. H. (2012). Realized GARCH: a joint model for returns and realized measures of volatility. *Journal of Applied Econometrics*, 27(6), 877–906.

- Held, M., Kapraun, J., Omachel, M., & Thimme, J. (2020). Up- and downside variance risk premia in global equity markets. *Journal of Banking & Finance*, 118, 105875.
- Heston, S. L. & Nandi, S. (2000). A closed-form GARCH option valuation model. *Review of Financial Studies*, 13(3), 585–625.
- Huang, Z., Tong, C., & Wang, T. (2019). VIX term structure and VIX futures pricing with realized volatility. *Journal of Futures Markets*, 39(1), 72–93.
- Huang, Z., Wang, T., & Hansen, P. R. (2017). Option pricing with the realized garch model: An analytical approximation approach. *Journal of Futures Markets*, 37(4), 328–358.
- Jiang, G. J. & Tian, Y. S. (2005). The model-free implied volatility and its information content. *The Review of Financial Studies*, 18(4), 1305–1342.
- Kilic, M. & Shaliastovich, I. (2019). Good and bad variance premia and expected returns. *Management Science*, 65(6), 2522–2544.
- Majewski, A. A., Borgetti, G., & Corsi, F. (2015). Smile from the past: A general option pricing framework with multiple volatility and leverage components. *Journal of Econometrics*, 187(2), 521–531.
- Patton, A. J. & Sheppard, K. (2015). Good Volatility, Bad Volatility: Signed Jumps and The Persistence of Volatility. *The Review of Economics and Statistics*, 97(3), 683–697.
- Qiao, G., Jiang, G., & Yang, J. (2022). Vix term structure forecasting: New evidence based on the realized semi-variances. *International Review of Financial Analysis*, 82, 102199.
- Schürger, K. (2002). Laplace transforms and suprema of stochastic processes. In *Advances in Finance and Stochastics* (pp. 285–294). Springer.
- Shephard, N. & Sheppard, K. (2010). Realising the future: forecasting with high-frequency-based volatility (HEAVY) models. *Journal of Applied Econometrics*, 25(2), 197–231.
- Tong, C., Hansen, P. R., & Huang, Z. (2022). Option pricing with state-dependent pricing kernel. *Journal of Futures Markets*, 42(8), 1409–1433.
- Tong, C. & Huang, Z. (2021). Pricing VIX options with realized volatility. *Journal of Futures Markets*, 41(8), 1180–1200.
- Wang, Q. & Wang, Z. (2021). VIX futures and its closed-form pricing through an affine GARCH model with realized variance. *Journal of Futures Markets*, 41(1), 135–156.

Wang, T., Shen, Y., Jiang, Y., & Huang, Z. (2017). Pricing the CBOE VIX futures with the Heston–Nandi GARCH model. *Journal of Futures Markets*, 37(7), 641–659.

Yang, X. & Wang, P. (2018). VIX futures pricing with conditional skewness. *Journal of Futures Markets*, 38(9), 1126–1151.

Zhu, S.-P. & Lian, G.-H. (2012). An analytical formula for VIX futures and its applications. *Journal of Futures Markets*, 32(2), 166–190.

A The correction terms in CBOE VIX

For function $\log(F)$ and any positive value $X_0 \geq 0$, we have

$$\mathbb{E}_0^{\mathbb{Q}}[\log(F_T)] - \log(X_0) = \mathbb{E}_0^{\mathbb{Q}}\left(\frac{F_T - X_0}{X_0}\right) - e^{rT} \left[\int_0^{X_0} \frac{P_0(K)}{K^2} dK + \int_{X_0}^{\infty} \frac{C_0(K)}{K^2} dK \right]$$

When X_0 is equal to the forward price F_0 , we obtain Equation (2), and the true MFIV is given by

$$\text{MFIV} \equiv 2e^{rT} \left[\int_0^{F_0} \frac{P_0(K)}{K^2} dK + \int_{F_0}^{\infty} \frac{C_0(K)}{K^2} dK \right] = -2\mathbb{E}_0^{\mathbb{Q}} \left[\log \frac{F_T}{F_0} \right]$$

However, if we choose X_0 as \tilde{F}_0 instead of F_0 , then the resulting $\widetilde{\text{MFIV}}$ is

$$\widetilde{\text{MFIV}} \equiv 2e^{rT} \left[\int_0^{\tilde{F}_0} \frac{P_0(K)}{K^2} dK + \int_{\tilde{F}_0}^{\infty} \frac{C_0(K)}{K^2} dK \right] = -2\mathbb{E}_0^{\mathbb{Q}} \left[\log \frac{F_T}{\tilde{F}_0} - \frac{F_T - \tilde{F}_0}{\tilde{F}_0} \right]$$

Then we have

$$\begin{aligned} \frac{1}{2} (\text{MFIV} - \widetilde{\text{MFIV}}) &= \mathbb{E}_0 \left(\frac{F_T - F_0}{F_0} - \log \frac{F_T}{F_0} \right) - \mathbb{E}_0 \left(\frac{F_T - \tilde{F}_0}{\tilde{F}_0} - \log \frac{F_T}{\tilde{F}_0} \right) \\ &= \log \left(\frac{F_0}{\tilde{F}_0} \right) - \left(\frac{F_0}{\tilde{F}_0} - 1 \right) \approx -\frac{1}{2} \left(\frac{F_0}{\tilde{F}_0} - 1 \right)^2 \end{aligned}$$

So we have

$$\text{MFIV} \approx \widetilde{\text{MFIV}} - \left(\frac{F_0}{\tilde{F}_0} - 1 \right)^2$$

and this forms the foundation of the correction term in calculating the CBOE VIX.

B Proof of Proposition 1

According to Equation (3), we have

$$\text{MFIV}_t \equiv 2e^{r(T-t)} \int_0^{+\infty} \frac{M_t(K)}{K^2} dK = -2\mathbb{E}_t^{\mathbb{Q}} \left[\log \left(\frac{F_T}{F_t} \right) \right] = -2\mathbb{E}_t^{\mathbb{Q}} \left[\sum_{i=1}^{T-t} (R_{t+i} - r) \right]$$

where the risk-neutral dynamics of log return R_{t+1} are given by

$$R_{t+1} = \bar{r}^* - \xi_u^* h_{u,t+1}^* - \xi_d^* h_{d,t+1}^* + z_{u,t+1}^* - z_{d,t+1}^*$$

Let $n = T - t$, then we have

$$\begin{aligned} \text{MFIV}_t &= -2\mathbb{E}_t^{\mathbb{Q}} \left[\sum_{i=1}^n (R_{t+i} - r) \right] \\ &= -2\mathbb{E}_t^{\mathbb{Q}} \left[\sum_{i=1}^n (\bar{r}^* - r - \xi_u^* h_{u,t+i}^* - \xi_d^* h_{d,t+i}^*) \right] \\ &= n \left[-2(\bar{r}^* - r) + 2\xi_u^* \mathbb{E}_t^{\mathbb{Q}} \left(\frac{1}{n} \sum_{i=1}^n h_{u,t+i}^* \right) + 2\xi_d^* \mathbb{E}_t^{\mathbb{Q}} \left(\frac{1}{n} \sum_{i=1}^n h_{d,t+i}^* \right) \right] \end{aligned}$$

Finally, the 1-month ahead (i.e. $n = 22$) VIX is given by

$$\text{VIX}_t = \frac{100\sqrt{252}}{22} \times \text{MFIV}_t = 100\sqrt{252} \times \sqrt{-2(\bar{r}^Q - r) + 2\xi_u^* V_{u,t}(22) + 2\xi_d^* V_{d,t}(22)}$$

where $V_{u,t}(n)$ and $V_{d,t}(n)$ are defined as

$$V_{j,t}(n) \equiv \frac{1}{n} \sum_{k=1}^n \mathbb{E}_t^{\mathbb{Q}} \left(h_{j,t+k}^* \right), \quad j = \{u, d\}$$

Now we can begin to derive the formula of $V_{j,t}(n)$. First, we rewrite the dynamics of $h_{j,t+1}^*$ as

$$\begin{aligned} h_{j,t+1}^* &= \omega_j^* + \beta_j (h_{j,t}^* - \omega_j^*) + \alpha_j^* \left(v_{j,t}^* - \gamma_j^* \sqrt{h_{j,t}^* - \omega_j^*} \right)^2 \\ &= \omega_j^* + \beta_j (h_{j,t}^* - \omega_j^*) + \alpha_j^* \left(v_{j,t}^{*2} + \gamma_j^{*2} (h_{j,t}^* - \omega_j^*) - 2\gamma_j^* v_{j,t}^* \sqrt{h_{j,t}^* - \omega_j^*} \right) \\ &= (\omega_j^* + \alpha_j^*) + (\beta_j + \alpha_j^* \gamma_j^{*2}) (h_{j,t}^* - \omega_j^*) + \alpha_j^* \left(v_{j,t}^{*2} - 1 - 2\gamma_j^* v_{j,t}^* \sqrt{h_{j,t}^* - \omega_j^*} \right) \end{aligned}$$

where the conditional expectation of the last innovation term is zero. So we have

$$\begin{aligned}
V_{j,t}(n) &= \bar{h}_j^* + \frac{1}{n} \sum_{k=1}^n (\beta_j + \alpha_j^* \gamma_j^{*2})^{k-1} (h_{j,t+1}^* - \bar{h}_j^*) \\
&= \bar{h}_j^* + \frac{1 - (\beta_j + \alpha_j^* \gamma_j^{*2})^n}{n [1 - (\beta_j + \alpha_j^* \gamma_j^{*2})]} (h_{j,t+1}^* - \bar{h}_j^*) \\
&= (1 - \Gamma_j(n)) \bar{h}_j^* + \Gamma_j(n) h_{j,t+1}^*
\end{aligned}$$

with

$$\Gamma_j(n) = \frac{1 - (\beta_j + \alpha_j^* \gamma_j^{*2})^n}{n [1 - (\beta_j + \alpha_j^* \gamma_j^{*2})]}, \quad \bar{h}_j^* = \frac{\omega_j^* + \alpha_j^*}{1 - (\beta_j + \alpha_j^* \gamma_j^{*2})} + \omega_j^*$$

□

C Proof of Proposition 2

Denote the future cumulative return by

$$\widetilde{R}_T \equiv \log \left(\frac{S_T}{S_0} \right) = \sum_{t=1}^T R_t, \quad R_t \equiv \log \left(\frac{S_t}{S_{t-1}} \right)$$

Because $F_t = S_t e^{r(T-t)}$, we have

$$\frac{F_T}{F_0} = \frac{S_T}{S_0} e^{-rT} = \exp \left(\sum_{t=1}^T R_t - rT \right) = \exp \left(\widetilde{R}_T - rT \right), \quad R_t \equiv \log \left(\frac{S_t}{S_{t-1}} \right)$$

C.1 Deriving the pricing formula of CIV^U

Then Equation (9) becomes

$$\begin{aligned}
\text{CIV}^U &= 2\mathbb{E}_0^{\mathbb{Q}} \left[\left(\frac{F_T}{F_0} - 1 - \ln \frac{F_T}{F_0} \right) \mathbb{I}_{\{F_T \geq F_0\}} \right] \\
&= 2\mathbb{E}_0^{\mathbb{Q}} \left[\left(e^{\widetilde{R}_T - rT} - 1 - \widetilde{R}_T + rT \right) \mathbb{I}_{\{\widetilde{R}_T - rT > 0\}} \right] \\
&= 2 \int_{rT}^{+\infty} (e^{R-rT} - 1 - R + rT) f(R) dR
\end{aligned} \tag{C.1}$$

where $f(R)$ is the conditional probability density function of future cumulative return \widetilde{R}_T in risk-neutral measure. By Fourier inverse transform, $f(R)$ can be expressed as

$$f(R) = \frac{1}{\pi} \int_0^{\infty} \Re [e^{-uR} \phi(u, T)] du_I, \quad \phi(u, T) \equiv \mathbb{E}_0^{\mathbb{Q}} [e^{uR}] \quad (\text{C.2})$$

where u is a complex number denoted by $u = u_R + iu_I$. The operator $\Re[\cdot]$ takes the real part of the complex number in the square brackets. Function $\phi(u, T)$ is the characteristic function of future cumulative returns \widetilde{R} . Combining Equations (C.1) and (C.2), we have

$$\text{CIV}^U = 2 \int_{rT}^{+\infty} (e^{R-rT} - 1 - R + rT) \frac{1}{\pi} \int_0^{\infty} \Re [e^{-uR} \phi(u, T)] du_I dR \quad (\text{C.3})$$

After using Fubini's theorem, we can change the order of integration. Then Equation (C.3) becomes

$$\text{CIV}^U = \frac{2}{\pi} \int_0^{\infty} \Re \left[\left(\int_{rT}^{+\infty} (e^{R-rT} - 1 - R + rT) e^{-uR} dR \right) \phi(u, T) \right] du_I$$

Under the condition of convergence that $u_R > 1$, the integral is

$$\begin{aligned} \int_{rT}^{+\infty} (e^{R-rT} - 1 - R + rT) e^{-uR} dR &= e^{-urT} \int_0^{+\infty} (e^s - 1 - s) e^{-us} ds \\ &= e^{-urT} \int_0^{\infty} (e^{(1-u)s} - e^{-us} - se^{-us}) ds \\ &= e^{-urT} \left(\frac{s}{u} e^{-us} + \frac{1}{1-u} e^{(1-u)s} + \frac{1}{u} e^{-us} + \frac{1}{u^2} e^{-us} \right) \Big|_0^{+\infty} \\ &= e^{-urT} \left(\frac{1}{u-1} - \frac{1}{u} - \frac{1}{u^2} \right) \end{aligned}$$

So we have

$$\text{CIV}^U = \frac{2}{\pi} \int_0^{\infty} \Re \left[e^{-urT} \left(\frac{1}{u-1} - \frac{1}{u} - \frac{1}{u^2} \right) \phi(u, T) \right] du_I$$

C.2 Deriving the pricing formula of CIV^D

Similar to Equation (C.3), we have

$$\text{CIV}^D = \frac{2}{\pi} \int_0^{\infty} \Re \left[\left(\int_{-\infty}^{rT} (e^{R-rT} - 1 - R + rT) e^{-uR} dR \right) \phi(u, T) \right] du_I$$

Under the condition of convergence that $u_R < 0$, the integral is

$$\begin{aligned}
\int_{-\infty}^{rT} (e^{R-rT} - 1 - R + rT) e^{-uR} dR &= e^{-urT} \int_{-\infty}^0 (e^s - 1 - s) e^{-us} ds \\
&= e^{-urT} \left(\frac{s}{u} e^{-us} + \frac{1}{1-u} e^{(1-u)s} + \frac{1}{u} e^{-us} + \frac{1}{u^2} e^{-us} \right) \Big|_{-\infty}^0 \\
&= e^{-urT} \left[\frac{1}{1-u} + \frac{1}{u} + \frac{1}{u^2} \right]
\end{aligned}$$

So we have

$$\text{CIV}^U = \frac{2}{\pi} \int_0^\infty \Re \left[e^{-urT} \left(\frac{1}{1-u} + \frac{1}{u} + \frac{1}{u^2} \right) \phi(u, T) \right] du$$

D Proof of Proposition 3

According to [Schürger \(2002\)](#), the expectation of the square root function of a random variable x can be expressed as

$$\mathbb{E}(\sqrt{x}) = \frac{1}{2\sqrt{\pi}} \int_0^\infty \frac{1 - \mathbb{E}(e^{-vx})}{v^{\frac{3}{2}}} dv$$

Using this identity, the VIX futures price can be written as

$$\begin{aligned}
F(t, T) &= \mathbb{E}_t^{\mathbb{Q}} [\text{VIX}_T] \\
&= \mathbb{E}_t^{\mathbb{Q}} \left[100\sqrt{252} \times \sqrt{-2(\bar{r}^* - r) + 2\xi_u^* V_{u,t}(22) + 2\xi_d^* V_{d,t}(22)} \right] \\
&= \frac{100\sqrt{252}}{2\sqrt{\pi}} \int_0^\infty \frac{1 - \mathbb{E}_t^{\mathbb{Q}} [\exp(2(\bar{r}^* - r)v - 2v\xi_u^* V_{u,t}(22) - 2v\xi_d^* V_{d,t}(22))]}{v^{3/2}} dv \\
&= \frac{50\sqrt{252}}{\sqrt{\pi}} \int_0^\infty \frac{1 - e^{2v(\bar{r}^* - r)} \Psi_{u,t}(-2v\xi_u^*, T) \Psi_{d,t}(-2v\xi_d^*, T)}{v^{3/2}} dv
\end{aligned}$$

where $\Psi_{j,t}(s, T)$ is the conditional MGF of $V_{j,T}(22)$ defined by

$$\Psi_{j,t}(s, T) = \mathbb{E}_t^{\mathbb{Q}} [\exp(sV_{j,T}(22))] ,$$

and the last equality comes from the assumption that shocks to upside and downside volatility, $v_{u,t}$ and $v_{d,t}$, respectively, are independent.

From [Feunou & Okou \(2019, Appendix A\)](#), the conditional MGF of $h_{j,t+2}^*$ is given by

$$\mathbb{E}_t^{\mathbb{Q}} [\exp(sh_{j,t+2}^*)] = \exp(A_j(s) + B_j(s)h_{j,t+1}^*)$$

with

$$A_j(s) = -\frac{1}{2} \log(1 - 2s\alpha_j^*) + s(\omega_j^* + \varpi_j^* - \omega_j^* \beta_j) - \frac{s\omega_j^* \alpha_j^* \gamma_j^{*2}}{1 - 2\alpha_j^* s}$$

$$B_j(s) = \frac{s\alpha_j^* \gamma_j^{*2}}{1 - 2s\alpha_j^*} + s\beta_j$$

Suppose that

$$\mathbb{E}_t^{\mathbb{Q}} [\exp(sV_{j,t+M}(n))] = \exp(H_j(s, M) + G_j(s, M) h_{j,t+1}^*)$$

when $M = 0$, we have

$$\mathbb{E}_t^{\mathbb{Q}} [\exp(sV_{j,t}(n))] = \exp(s(1 - \Gamma_j(n)) \bar{h}_j^* + s\Gamma_j(n) h_{j,t+1}^*)$$

$$H_j(s, 0) = s(1 - \Gamma_j(n)) \bar{h}_j^*, \quad G_j(s, 0) = s\Gamma_j(n)$$

for $M = M + 1$, we have

$$\begin{aligned} \mathbb{E}_t^{\mathbb{Q}} [\exp(sV_{j,t+M+1}(n))] &= \mathbb{E}_t^{\mathbb{Q}} [\mathbb{E}_{t+1}^{\mathbb{Q}} \exp(sV_{j,t+M+1}(n))] \\ &= \mathbb{E}_t^{\mathbb{Q}} [\exp(H_j(s, M) + G_j(s, M) h_{j,t+2}^*)] \\ &= \exp(H_j(s, M) + A_j(G_j(s, M)) + B_j(G_j(s, M)) h_{j,t+1}^*) \\ &= \exp(H_j(s, M+1) + G_j(s, M+1) h_{j,t+1}^*) \end{aligned}$$

with

$$H_j(s, M+1) = H_j(s, M) + A_j(G_j(s, M))$$

$$G_j(s, M+1) = B_j(G_j(s, M))$$

E The measurement equation of the GSARV model in \mathbb{Q} -measure

According to [Feunou & Okou \(2019, Appendix C\)](#), the measurement equation in \mathbb{Q} -measure is given by

$$\begin{aligned}
 RV_{j,t} &= h_{j,t} + \frac{\sigma_j}{\kappa_2^j} \left[\left(v_{j,t}^* - \gamma_j^* \sqrt{h_{j,t}^* - \omega_j^*} \right)^2 - \kappa_2^j (1 + \gamma_j^2 (h_{j,t} - \omega_j)) \right] \\
 &= h_{j,t} + \frac{\sigma_j}{\kappa_2^j} \left(v_{j,t}^* - \gamma_j^* \sqrt{h_{j,t}^* - \omega_j^*} \right)^2 - \sigma_j - \sigma_j \gamma_j^2 h_{j,t} + \sigma_j \gamma_j^2 \omega_j \\
 &= (1 - \sigma_j \gamma_j^2) h_{j,t} + \sigma_j \gamma_j^2 \omega_j - \sigma_j + \frac{\sigma_j}{\kappa_2^j} \left(v_{j,t}^* - \gamma_j^* \sqrt{h_{j,t}^* - \omega_j^*} \right)^2 \\
 &= (1 - \sigma_j \gamma_j^2) h_{j,t} + \sigma_j \gamma_j^2 \omega_j - \sigma_j + \frac{\sigma_j}{\kappa_2^j} [1 + \gamma_j^{*2} (h_{j,t}^* - \omega_j^*)] + \frac{\sigma_j}{\kappa_2^j} \tilde{\varepsilon}_{j,t}
 \end{aligned}$$

where $\tilde{\varepsilon}_{j,t}$ is a zero-mean innovation defined by

$$\tilde{\varepsilon}_{j,t} = \left[\left(v_{j,t}^* - \gamma_j^* \sqrt{h_{j,t}^* - \omega_j^*} \right)^2 - 1 - \gamma_j^{*2} (h_{j,t}^* - \omega_j^*) \right]$$

As $h_{j,t}^*$ can be written as $h_{j,t}^* = \vartheta_j + \zeta_j h_{j,t}$, the formula above becomes

$$\begin{aligned}
 RV_{j,t} &= (1 - \sigma_j \gamma_j^2) \frac{h_{j,t}^* - \vartheta_j}{\zeta_j} + \sigma_j \gamma_j^2 \omega_j - \sigma_j + \frac{\sigma_j}{\kappa_2^j} [1 + \gamma_j^{*2} (h_{j,t}^* - \omega_j^*)] + \frac{\sigma_j}{\kappa_2^j} \tilde{\varepsilon}_{j,t} \\
 &= A_j^* + B_j^* h_{j,t}^* + \frac{\sigma_j}{\kappa_2^j} \tilde{\varepsilon}_{j,t}
 \end{aligned}$$

where

$$A_j^* = \sigma_j \gamma_j^2 \omega_j - \sigma_j - \frac{\vartheta_j}{\zeta_j} (1 - \sigma_j \gamma_j^2) + \frac{\sigma_j}{\kappa_2^j} (1 - \gamma_j^{*2} \omega_j^*), \quad B_j^* = \frac{1 - \sigma_j \gamma_j^2}{\zeta_j} + \frac{\sigma_j}{\kappa_2^j} \gamma_j^{*2}$$

Define

$$\zeta_j^* = -\frac{A_j^*}{B_j^*}, \quad \phi_j^* = \frac{1}{B_j^*}, \quad \sigma_j^* = \frac{\sigma_j}{B_j^* \kappa_2^j}$$

Then we have

$$RV_{j,t}^* \equiv \zeta_j^* + \phi_j^* RV_{j,t} = h_{j,t}^* + \sigma_j^* \tilde{\varepsilon}_{j,t}$$